Electronic Supplementary Material (ESI) for CrystEngComm.

Electronic Supplemental Information

For

Quinoxaline-annulated hexadehydro[12]annulene: Use of a new building block to construct a hydrogen-bonded hexagonal molecular network

Mayu Kobayashi, Haruka Kubo, Ryusei Oketani, Ichiro Hisaki*

Department of Chemistry, Graduate School of Engineering Science, Osaka University

Contents

1. General.

All reagents and solvents were used as received from commercial suppliers. ^{1}H NMR spectra were measured by a JEOL 400 YH (400 MHz) or Bruker AV400M (400 MHz) spectrometer. Residual protons and carbons of deuterated solvents were used as internal standards for the measurements: δ = 7.26 ppm ($CDCl_3$) and 2.50 ppm (DMSO-d_6) for ^{1}H NMR and δ = 77.0 ppm ($CDCl_3$) and 29.76 ppm (DMSO-d_6) for ^{13}C NMR. Thermogravimetric (TG) analysis was performed on Rigaku TG8120 under an N_2 purge (300 mL/min) at a heating rate of 5 K min^{-1}. Fluorescence and excitation spectra were measured on JASCO FP-8500 spectrofluorometer. Fluorescence quantum yields in a solution state and solid state were determined with JASCO FP-8500 equipping integrating sphere. HR-MS analysis was performed on a JEOL JMS-700 or JMS-S3000 MALDI-Spiral-TOFMS spectrometer. Theoretical calculation was performed on Gaussian 09.[S1] Molecular structures were optimized by DFT method at B3LYP/6-311+G** level. Electron transition was calculated by TD-DFT at B3LYP/6-311+G** level with polarizable continuum model. NICS values were calculated by GIAO/B3LYP/6-31G*. Powder X-ray diffraction (PXRD) data were collected on a Rigaku Ultima-IV (40 kV, 44 mA) using graphite-monochromatized Cu-Kα radiation at room temperature. A scan rate is 2.0° min^{-1}.

Single crystal X-ray measurement and analysis. Diffraction data of **TQ12-1(MeBz)** was collected on a two-dimensional X-ray detectors (PILATUS 200K/R) equipped in Rigaku XtaLAB P200 diffractometer using multi-layer mirror monochromated Cu-Kα radiation (λ = 1.54187 Å). All calculations were performed with the observed reflections [I > 2σ(I)] with the program CrystalStructure ver4.3. The initial structure was obtained by SHEXT[S2] and structural refinement was performed by SHELXL.[S3] All non-hydrogen atoms except for highly disordered solvent molecules accommodated in voids were refined with anisotropic displacement parameters, and hydrogen atoms were placed in idealized positions and refined as rigid atoms with the relative isotropic displacement parameters. SQUEEZE function equipped in the PLATON program was used to remove severely disordered solvent molecules in voids.[S4] Variable temperature (VT) PXRD measurement was performed on a Rigaku Ultima-IV using graphite-monochromatized Cu-Kα radiation with a temperature control unit under ambient atmosphere. Temperature of the sample was increased from room temperature to 360 °C with a rate of 1.0 °C min^{-1}. During temperature increasing, XRD patterns ranged from 2.0° to 22° was repeatedly recorded with a scan rate of 4° min^{-1}. Therefore, each PXRD scan has a temperature width of ca. 5 °C.

2. Synthesis

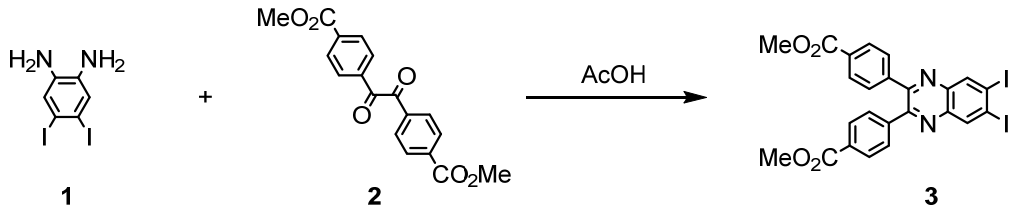

Diidoquinoxaline derivative 3. 4,5-Diamino-1,2-diiodobenzene (**1**) (1.03 g, 2.86 mmol) and dimethyl 4,4'-oxalyldibenzoate (**2**) (1.04 g, 3.19 mmol) in acetyl acid (100 mL) was stirred for 48 h at 75 °C to give dark yellow suspension. After cooling to rt, the precipitate was collected by filtration, washed with water to yield **3** (1.85 g, 99%) as a pale white solid.

3. Mp. >300 °C. ^{1}H NMR ($CDCl_3$, 400 MHz) δ 8.77 (s, 2H), 8.02-7.99 (m, 4H), 7.57-7.54 (m, 4H), 3.93 (s, 6H) ppm. ^{13}C NMR ($CDCl_3$, 100 MHz) δ 166.4, 153.2, 142.3, 140.8, 139.4, 130.8, 129.8, 129.7, 110.2, 52.3 ppm. HR-MS (FAB) *m/z* calcd. for $[M+H]^+$ $C_{24}H_{17}I_2N_2O_4$: 650.9278; found: 650.9294.

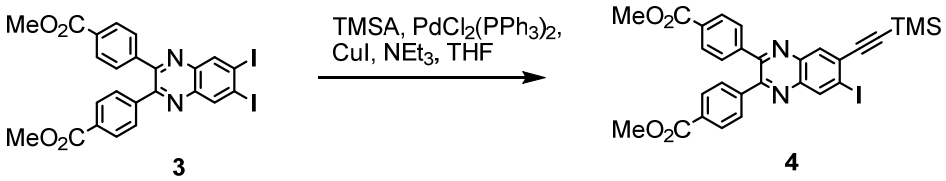

Trimethylsilylethynylquinoxyaline derivative 4. To a mixture of Diiodoquinoxaline derivative **3** (1.80 g, 2.77 mmol), $PdCl_2(PPh_3)_2$ (300 mg, 0.427 mmol), CuI (154 mg, 0.809 mmol), and Et_3N (50 mL) in deoxygenated THF (100 mL) was added trimethylsilylacetylene (500 mL, 3.51 mmol) dropwise at rt. After stirring for 24 h at room temperature, the reaction mixture was evaporated and passed through a bed of silica gel with CH_2Cl_2 and then with AcOEt. The product was purified by preparative HPLC with $CHCl_3$, followed by rinsing the resultant solid with diethyl ether to give **4** (615 mg, 36%) as a white solid.

Mp. 238–244 °C. ^{1}H NMR ($CDCl_3$, 400 MHz) δ 8.74 (s, 1H), 8.27 (s, 1H), 8.01 (d, J = 8.4 Hz, 4H), 7.57-7.55 (m, 4H), 3.93 (s, 6H), 0.34 (9H) ppm. ^{13}C NMR ($CDCl_3$, 100 MHz) δ 166.48, 166.46, 153.2, 152.9, 142.48, 142.40, 141.1, 140.4, 139.4, 132.6, 131.3, 130.8, 130.7, 129.9, 129.8, 129.6 (2C), 105.5, 102.9, 102.5, 52.3, −0.3 ppm. HR-MS (FAB) *m/z* calcd. for $[M+H]^+$ $C_{29}H_{26}IN_2O_4Si$: 621.0707; found: 621.0700.

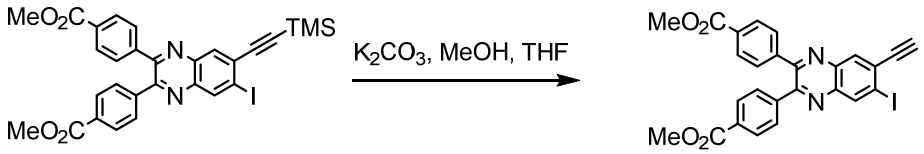

4 4a

Terminal acetylene 4a. A suspension of trimethylsilylethynyl quinoxaline derivative **4** (405 mg, 0.653 mmol) and K_2CO_3 (0.901 g, 6.52 mmol) in a mixed solvent of THF (50 mL) and MeOH (50 mL) was stirred for 3 h at room temperature. The product was extracted with CH_2Cl_2, washed with water and brine, dried over anhydrous $MgSO_4$, and concentrated to yield **4a** as a brown solid, which was used for the following reaction without further purification.

4a. ^{1}H NMR (400 MHz, $CDCl_3$) δ 8.76 (s, 1H), 8.32 (s, 1H), 8.01 (d, J = 8.0 Hz, 4H), 7.58-7.55 (m, 4H), 3.93 (s, 6H), 3.61 (s, 1H) ppm. ^{13}C NMR (100 MHz, $CDCl_3$) δ 166.46, 153.4, 153.3, 142.4, 142.3, 141.3, 140.3, 139.6, 133.7, 130.9, 130.8, 130.4, 129.9, 129.8, 129.7, 101.8, 84.3, 83.8, 52.3 ppm. HR-MS (FAB) *m/z* calcd. for $[M+H]^+$ $C_{26}H_{18}IN_2O_4$: 549.0311; found: 549.0322.

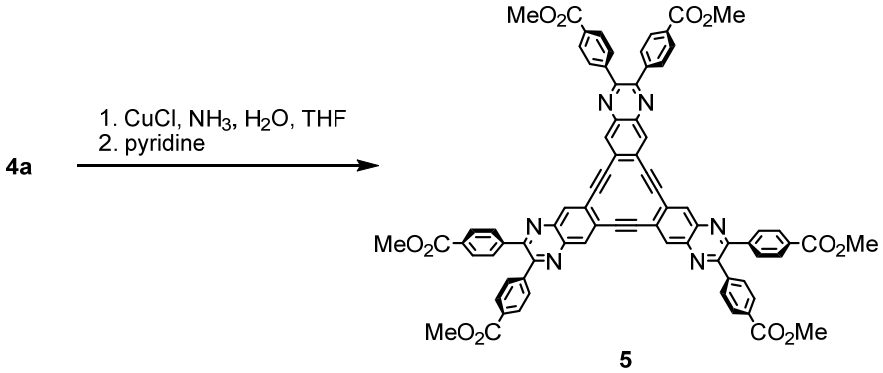

5

Hexadehydrotrisquinoxalino[12]annulene derivative 5. To a solution of $CuCl_2$ (439 mg, 3.27 mmol) dissolved in 30%-NH_3 aqueous solution (100 mL) was added dropwise the above-synthesized terminal acetylene dissolved in THF (100 mL). After stirring at room temperature for 2 h, the resultant orange precipitate was collected by centrifuge, washed with water, and dried *in vacuo* to give an acetylide. The acetylide was dissolved in pyridine (40 mL) and stirred at 120 °C for 12 h. After removing pyridine *in vacuo*, the product was purified by column chromatography (silica gel, $CHCl_3$ to 1%-Et_3N contained $CHCl_3$/AcOEt), followed by rinse with AcOEt to give **5** (38.8 mg, 14% from **4** in 2 steps) as a yellow solid.

5. Mp. >300 °C. ^{1}H NMR (400 MHz, $CDCl_3$) δ 8.39 (s, 6H), 8.02 (d, J = 8.0 Hz, 12H), 7.58 (d, J = 8.4 Hz, 12H), 3.95 (s, 18H) ppm. ^{13}C NMR (100 MHz, $CDCl_3$) δ 166.4, 153.5(br), 142.4(br), 141.1(br), 133.6, 130.9, 129.90, 129.67, 126.9, 93.8, 52.4 ppm. HR-MS (FAB) *m/z* calcd. for $[M]^+$ $C_{78}H_{48}N_6O_{12}$: 1260.3330; found: 1260.3311.

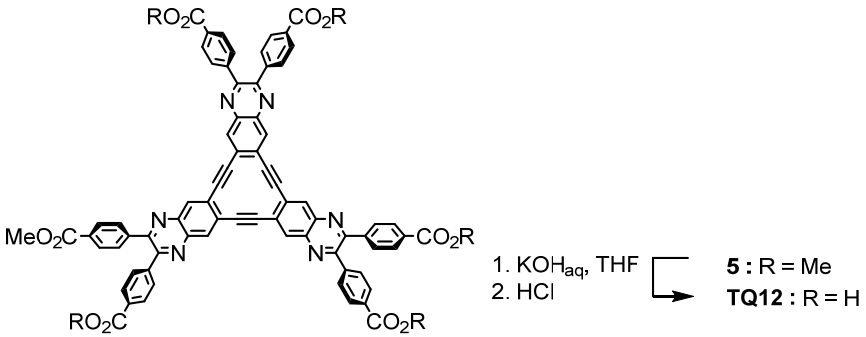

TQ12. To a solution of methyl ester derivative **5** (38 mg, 0.030 mmol) dissolved in THF (20 mL) was added KOH (100 mg, 1.78 mmol) dissolved in water (30 mL). The reaction mixture was stirred at 45 °C for 12 h. After removing THF *in vacuo*, the resultant aqueous solution was neutralized with 10%-HCl aqueous solution to yield orange suspension. To the suspension was added a saturated NaCl aqueous solution, and the product was collected by centrifuge, rinsed with water, and dried in vacuo to give **TQ12** (36 mg, quant.) as an orange solid.

TQ12. M.p. 295 °C (decomp.), ^{1}H NMR (400 MHz, DMSO-d_6) δ 8.11 (s, 6H), 7.90 (br.d, J = 6.8 Hz, 12H), 7.39 (br.d, J = 6.8 Hz, 12H) ppm. ^{13}C NMR (100 MHz, $CDCl_3$) δ 167.2, 153.5, 142.0, 140.9, 131.7, 130.4 (2C), 129.4, 126.3, 93.7 ppm. HR-MS (MALDI) *m/z* calcd. for $[M]^+$ $C_{72}H_{36}N_6O_{12}$: 1176.2391; found: 1176.2386.

3. Theoretical Calculation

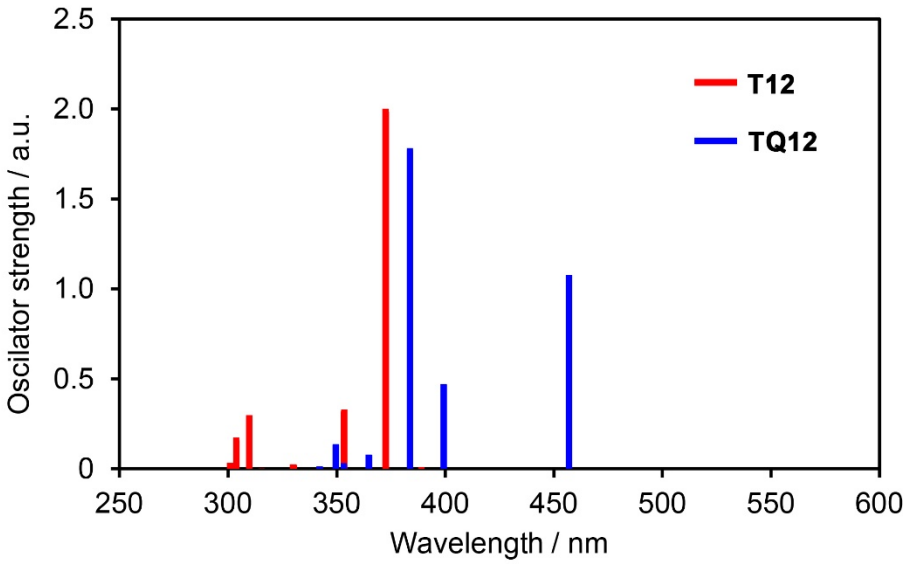

Fig. S1 Theoretical electron transition of **TQ12** (blue) and **T12** (red). TD-DFT calculation was performed at the B3LYP/6-311+G(p,d) level of theory with polarizable continuum model (DMSO).

4. Crystallography

TQ12 (6.5 mg) was dissolved in dimethylacetamide (1.5 mL) at 120 °C. To the hot solution was added dropwise methyl benzoate (2.5 mL). The mixed solution was filtered and placed at 90 °C for a couple days to yield columnar shaped single crystals suitable for X-ray crystallographic analysis.

Table S1. Crystal data of **TQ12-1(MeBz)**

Formula[a]	$2(C_{72}H_{36}N_6O_{12})\cdot 8(C_8H_8O_2)\cdot(C_4H_9NO)$
Formula weight	3530.54
Crystal system	Monoclinic
Space group	*C2/c*
a / Å	49.9843(13)
b / Å	28.7291(6)
c / Å	26.9217(8)
α / deg.	90
β / deg.	96.118(2)
γ / deg.	90
V/ Å^3	38439.5(17)
Z / Z'	16 / 2
T / K	213
Refln. obs.	96951
Refln. Uniq.	37445
R / wR	0.0857 / 0.2855
Completeness	0.95
GOF	0.987
CCDC no.	2159883

[a] The component ratio was determined based on electron numbers found in the solvent accessible void in the unit cell and on solvent accessible volume in the unit cell and molecular volumes of MeBz and DMA.

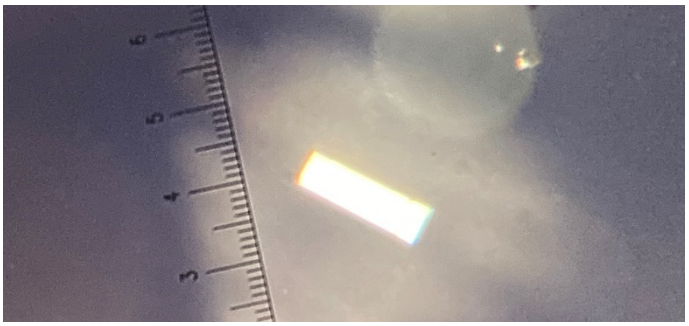

Fig. S2 Photograph of a single crystals of HOF **TQ12-1(MeBz)**

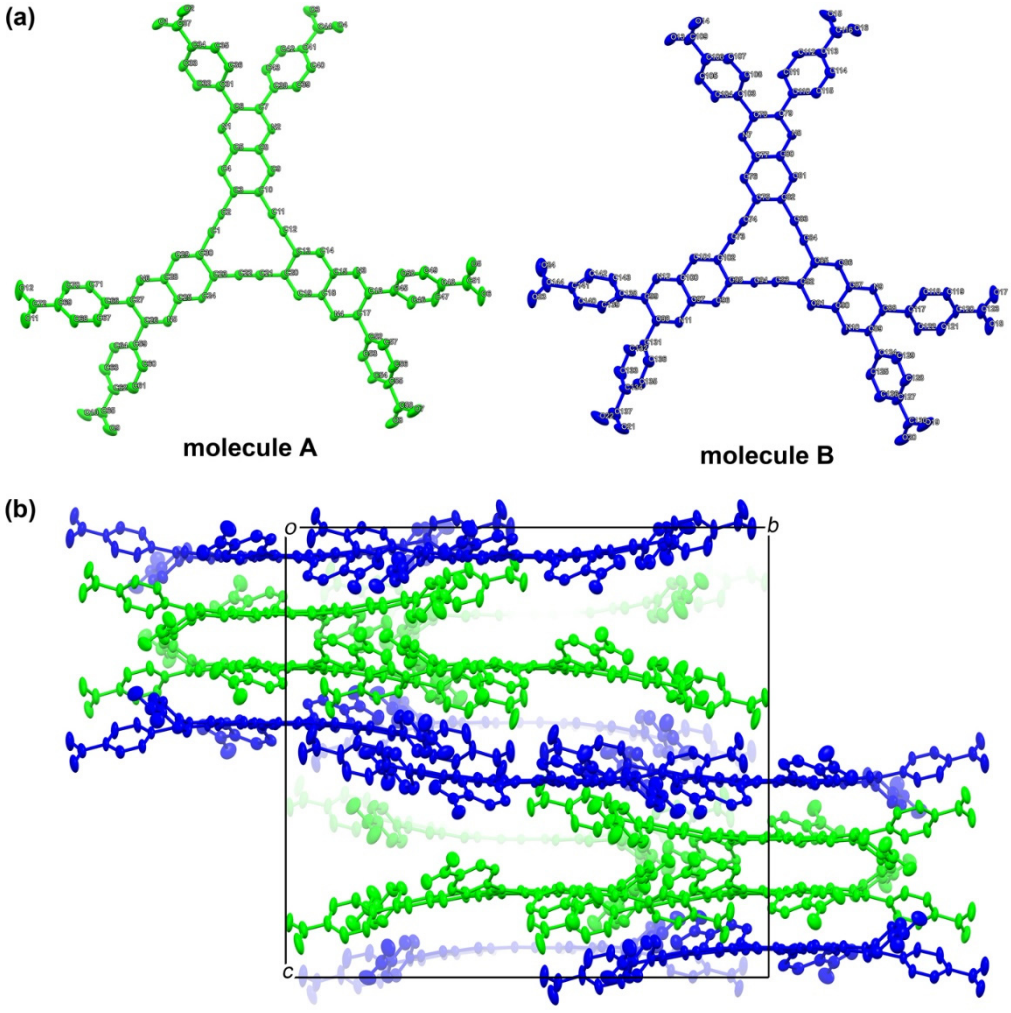

Fig. S3 (a) Crystallographicaly independent two molecules A and B colored with green and blue, respectively. (b) Packing diagram of the unit cell of **TQ12-1(MeBz)**.

5. Thermal analysis

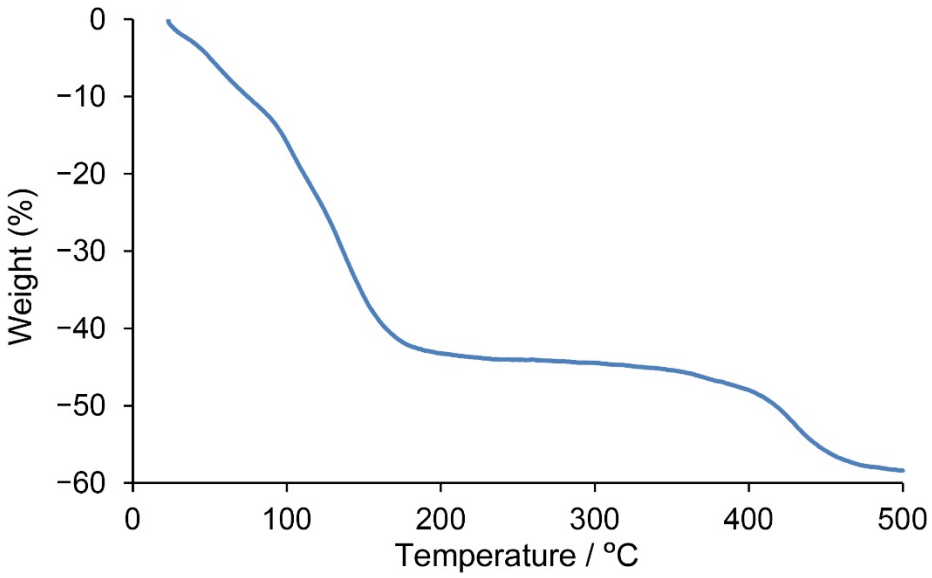

Fig. S4 TG analysis of **TQ12-1(MeBz)**.

The included solvent molecules were removed completely at 200 °C. TG analysis provided a component ratio of **TQ12** : MeBz : DMA = 2 : 12 : 1, which was however, unacceptable when considering volume of void calculated from the crystal structure. The amount of methyl benzoate molecule included in the void was overestimated due to high-boiling liquid (i.e. methyl benzoate) remaining on surface of aggregated crystalline particles, as often observed in the case of crystalline precipitates with small particle sizes formed from mother liquid with highly boiling point.

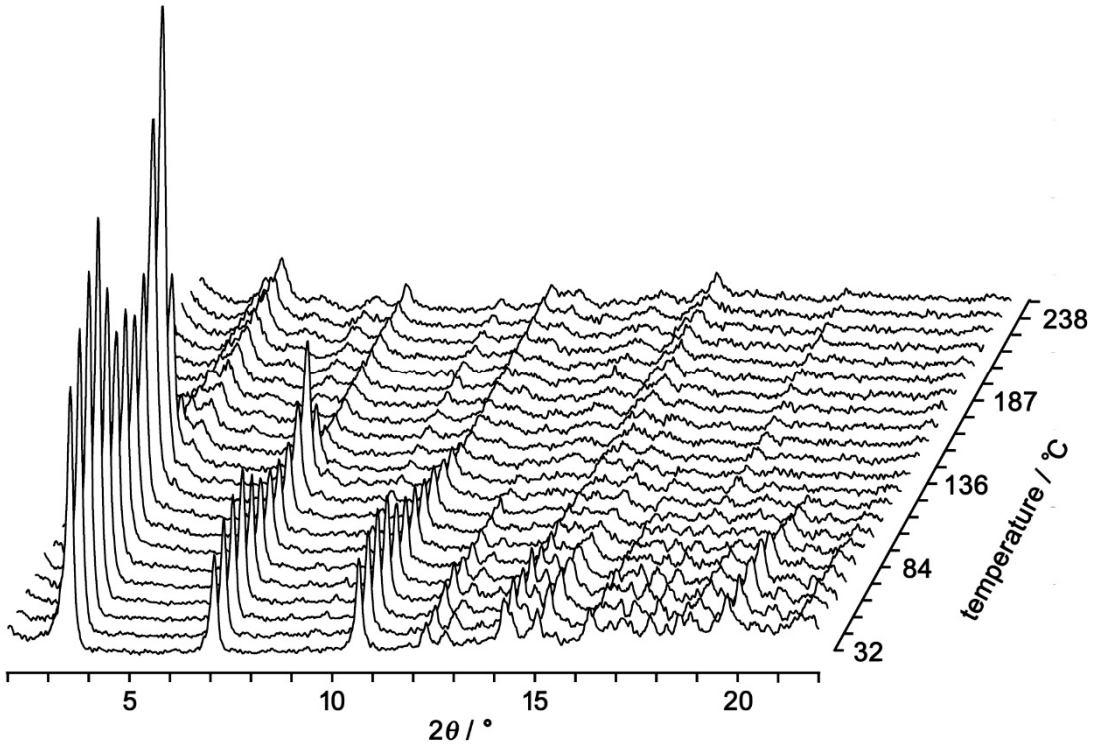

Fig. S5 Variable temperature PXRD patterns of **TQ12-1(MeBz)**. The initially observed pattern was drastically decayed at 146 °C.

6. Photophysical property in a solution state

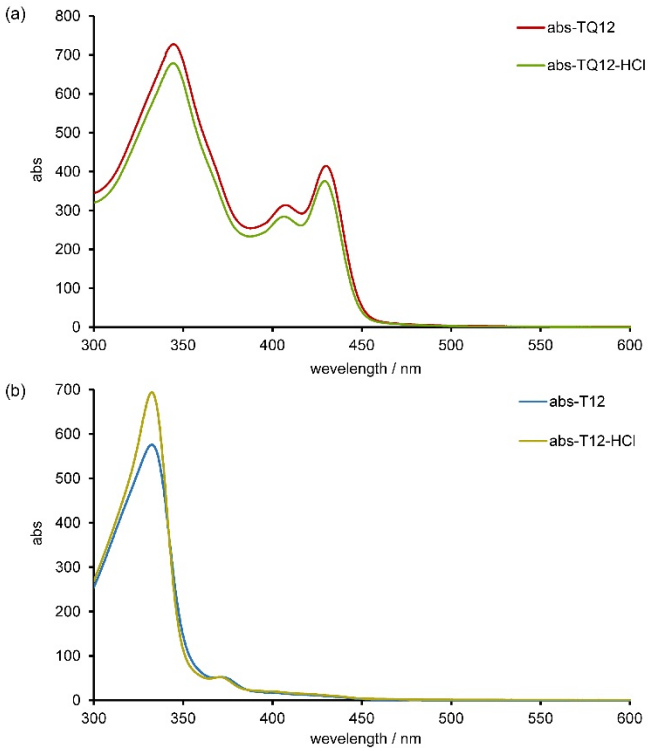

Fig. S6 UV-vis spectra of (a) **TQ12** and (b) **T12** before and after introducing HCl fume in DMSO solutions. Upon exposing to HCl fume no new absorption band appeared either in the case of **TQ12** and **T12**.

The UV-vis spectrum of the solution showed no changes upon exposing to HCl fume. This is probably caused from deep solvation by solvent DMSO molecules, which was also observed in previously reported **CPHATN** system.[S5]

7. Atomic coordinates

Table S2. Atomic coordinates of **T12**.

Atomic Number	Coordinates (Angstroms) X	Y	Z
C	0.000000	0.000000	0.000000
C	2.835744	0.000000	0.000000
C	0.710517	1.230404	0.000000
C	0.730066	-1.194426	0.014397
C	2.127834	-1.225677	0.022424
C	2.110037	1.195042	-0.003090
H	0.183560	-2.128603	0.053918
H	2.646355	2.135153	-0.041593
C	0.021091	2.470583	-0.017218
C	-0.584837	3.518261	-0.010187
C	-1.418827	-0.023011	0.007373
C	2.793514	-2.555646	0.103263
C	3.963198	-5.104718	0.297305
C	3.730457	-2.839326	1.108493
C	2.450695	-3.573128	-0.798832
C	3.030661	-4.833389	-0.709238
C	4.305202	-4.098070	1.207472
H	3.998243	-2.071388	1.823792
H	1.735627	-3.368589	-1.587676
H	2.765317	-5.606639	-1.418157
H	5.021160	-4.321209	1.988777
C	4.320993	0.087563	-0.069681
C	7.115078	0.345768	-0.242919
C	5.024333	0.896554	0.834415
C	5.042395	-0.586978	-1.066388
C	6.420712	-0.457025	-1.155125
C	6.406551	1.022751	0.755128
H	4.484059	1.417543	1.616780
H	4.516297	-1.205528	-1.783138
H	6.977618	-0.969469	-1.929776
H	6.938393	1.641777	1.465655
C	8.591043	0.448999	-0.377943
O	9.249980	-0.102943	-1.227921
O	9.155955	1.243795	0.567567
C	4.609461	-6.434513	0.443315
O	5.410959	-6.725788	1.300028
O	4.208501	-7.325699	-0.500143
C	-1.314139	4.735425	-0.026163
C	-2.730972	7.191740	-0.046855
C	-2.734975	4.736161	-0.017617
C	-0.644239	5.964654	-0.030435
C	-1.315438	7.191101	-0.032903
C	-3.403592	5.966113	-0.031256
H	0.438292	5.958379	0.001544
H	-4.486107	5.960617	-0.064182

Table S2. Continued

C	-3.465011	3.519280	-0.017669
C	-0.495502	8.433065	0.028080
C	1.129147	10.722071	0.184783
C	-0.712090	9.398609	1.022902
C	0.551900	8.633409	-0.882618
C	1.354226	9.766512	-0.811524
C	0.091655	10.526457	1.103533
H	-1.506945	9.255637	1.744607
H	0.727592	7.902269	-1.663634
H	2.152429	9.914271	-1.527020
H	-0.068278	11.267629	1.876785
C	-3.549246	8.433703	-0.126914
C	-5.170117	10.722696	-0.318572
C	-4.595078	8.650611	0.781784
C	-3.332412	9.382504	-1.137616
C	-4.134313	10.510297	-1.235468
C	-5.395530	9.783817	0.693400
H	-4.770827	7.932490	1.574790
H	-2.538964	9.226246	-1.858111
H	-3.974245	11.238423	-2.020981
H	-6.192513	9.944639	1.407444
C	-5.997844	11.947915	-0.463608
O	-5.854180	12.784028	-1.324694
O	-6.962890	12.051787	0.486633
C	1.959057	11.947884	0.311145
O	1.816470	12.797584	1.159069
O	2.924628	12.035148	-0.640122
C	-4.758662	1.230450	0.005358
C	-6.175453	-1.226094	0.014042
C	-4.047877	0.000175	-0.002102
C	-6.158190	1.194741	0.008515
C	-6.883672	-0.000445	0.004204
C	-4.777738	-1.194474	0.002305
H	-6.694843	2.135005	-0.020292
H	-4.230975	-2.128897	0.031281
C	-2.629034	-0.022822	-0.007476
C	-4.069849	2.471128	0.003256
C	-8.369206	0.087258	-0.059306
C	-11.164023	0.345907	-0.219837
C	-9.094147	-0.579119	-1.058907
C	-9.069440	0.888295	0.854229
C	-10.451965	1.014718	0.781177
C	-10.472825	-0.448872	-1.141398
H	-8.570567	-1.191278	-1.782931
H	-8.526344	1.402652	1.639031
H	-10.981441	1.627512	1.498836
H	-11.032428	-0.954898	-1.918320
C	-6.840783	-2.556790	0.084815
C	-8.010035	-5.107527	0.258779
C	-6.502012	-3.565369	-0.828711
C	-7.773408	-2.850268	1.091233

Table S2. Continued

C	-8.347807	-4.109896	1.180395
C	-7.081864	-4.826368	-0.749089
H	-5.790353	-3.353142	-1.618610
H	-8.037870	-2.089421	1.815290
H	-9.060305	-4.340672	1.962646
H	-6.819776	-5.592571	-1.466819
C	-8.655788	-6.438667	0.394461
O	-9.453484	-6.738410	1.251804
O	-8.259476	-7.320288	-0.559865
C	-12.640518	0.449694	-0.348358
O	-13.302614	-0.096049	-1.199829
O	-13.201998	1.237415	0.605202
H	4.681485	-8.151675	-0.321771
H	-8.731790	-8.147958	-0.387676
H	-14.155819	1.240158	0.437910
H	-7.441699	12.874433	0.308410
H	3.404706	12.859770	-0.474927
H	10.109179	1.245372	0.396902

Table S3. Atomic coordinates of **TQ12**

Atomic Number	Coordinates (Angstroms) X	Y	Z
C	1.829738	4.904579	0.093832
C	0.935034	7.463488	0.051000
C	0.441209	5.216019	0.079371
N	2.753554	5.892857	0.181280
C	2.341550	7.145367	0.206079
N	0.027984	6.506336	0.034629
C	3.398829	8.165074	0.447597
C	5.465361	9.989122	0.961939
C	3.210760	9.214965	1.357793
C	4.640276	8.032495	-0.188993
C	5.661574	8.941437	0.054652
C	4.236173	10.112985	1.618200
H	2.266139	9.321751	1.876394
H	4.795621	7.208570	-0.873997
H	6.612829	8.840181	-0.450887
H	4.101246	10.918119	2.329578
C	0.415655	8.844559	-0.146032
C	-0.671838	11.392243	-0.580748
C	-0.770190	9.231006	0.493102
C	1.041978	9.745946	-1.018580
C	0.499435	11.003916	-1.239685
C	-1.304596	10.496450	0.288992
H	-1.268618	8.527913	1.148412
H	1.946991	9.458446	-1.539096
H	0.971377	11.699546	-1.922231
H	-2.213457	10.792116	0.796205
C	-1.205049	12.755341	-0.842457
O	-0.706944	13.561238	-1.592952
O	-2.336554	13.024859	-0.142642
C	6.526787	10.984751	1.266563
O	6.415232	11.897759	2.050654
O	7.669362	10.772466	0.564882
C	-0.506939	4.170383	0.065593
H	-1.558706	4.426459	0.056384
C	2.240970	3.554589	0.062932
H	3.301352	3.336932	0.072403
C	1.310594	2.529274	0.036404
C	-0.103176	2.845904	0.048449
C	-1.065122	1.804531	0.026296
C	1.735911	1.176897	0.014064
C	-5.161632	-0.867622	0.001766
C	-6.928470	-2.922957	0.060738
C	-4.736748	-2.225799	-0.012736
N	-6.481244	-0.561075	-0.047960
C	-7.360107	-1.544124	-0.063954
N	-5.646109	-3.229757	0.040743
C	-8.777733	-1.135492	-0.262554
C	-11.404893	-0.255234	-0.693433

Table S3. Continued

C	-9.615751	-1.810322	-1.160158
C	-9.267589	-0.003120	0.404173
C	-10.570899	0.425852	0.200597
C	-10.915226	-1.371078	-1.381067
H	-9.248753	-2.673360	-1.701595
H	-8.614125	0.534651	1.079429
H	-10.959537	1.291433	0.722604
H	-11.551520	-1.890103	-2.085492
C	-7.859509	-4.066557	0.264234
C	-9.514121	-6.286959	0.705039
C	-7.619552	-5.276781	-0.402473
C	-8.928488	-3.988932	1.166776
C	-9.744577	-5.090434	1.392749
C	-8.444917	-6.371976	-0.194008
H	-6.779205	-5.346882	-1.081507
H	-9.116288	-3.070130	1.708283
H	-10.559700	-5.026190	2.101206
H	-8.273215	-7.305174	-0.715947
C	-10.367353	-7.489232	0.897552
O	-10.217490	-8.543301	0.325313
O	-11.362130	-7.294072	1.800376
C	-12.792064	0.245847	-0.880856
O	-13.266993	1.199060	-0.309084
O	-13.502445	-0.484003	-1.778235
C	-3.357193	-2.523827	-0.036472
H	-3.052956	-3.562645	-0.049625
C	-4.197754	0.163456	0.022393
H	-4.539680	1.190486	0.035614
C	-2.844391	-0.129472	0.009121
C	-2.412017	-1.511888	-0.025558
C	-1.029103	-1.823707	-0.048735
C	-1.885458	0.914692	0.030859
C	3.332851	-4.034907	-0.095414
C	5.994015	-4.538587	-0.214962
C	4.296932	-2.988170	-0.106229
N	3.727784	-5.330947	-0.051877
C	5.018460	-5.601248	-0.065208
N	5.619391	-3.274385	-0.189756
C	5.376970	-7.033026	0.128145
C	5.935877	-9.747785	0.551837
C	6.400127	-7.420320	1.003593
C	4.625633	-8.024154	-0.519846
C	4.909381	-9.367138	-0.319940
C	6.673573	-8.765081	1.220887
H	6.976604	-6.670317	1.530712
H	3.818538	-7.727951	-1.177893
H	4.342120	-10.137125	-0.827956
H	7.457103	-9.055999	1.907830
C	7.445043	-4.774048	-0.450334
C	10.185287	-5.095958	-0.950769
C	8.386674	-3.957927	0.191043

Table S3. Continued

C	7.893161	-5.743619	-1.358801
C	9.248849	-5.897760	-1.612062
C	9.745053	-4.122815	-0.046027
H	8.041470	-3.192259	0.874272
H	7.180295	-6.369136	-1.881440
H	9.600041	-6.636128	-2.321995
H	10.466536	-3.497248	0.462750
C	11.626368	-5.310419	-1.246890
O	12.059563	-6.130128	-2.022366
O	12.440484	-4.478969	-0.547569
C	6.198903	-11.199601	0.735994
O	5.596715	-12.087991	0.180101
O	7.206761	-11.448668	1.610416
C	3.866144	-1.644299	-0.075132
H	4.613828	-0.861484	-0.082294
C	1.957940	-3.715396	-0.084018
H	1.239254	-4.524915	-0.077368
C	1.535609	-2.396746	-0.065843
C	2.517412	-1.331376	-0.051058
C	2.096784	0.022448	-0.028504
C	0.151849	-2.088466	-0.044633
H	-2.603573	13.925222	-0.379147
H	8.292699	11.464512	0.830217
H	13.348361	-4.692948	-0.808045
H	7.301310	-12.411134	1.661398
H	-11.855857	-8.125322	1.856333
H	-14.382203	-0.082642	-1.831195

8. NMR spectra

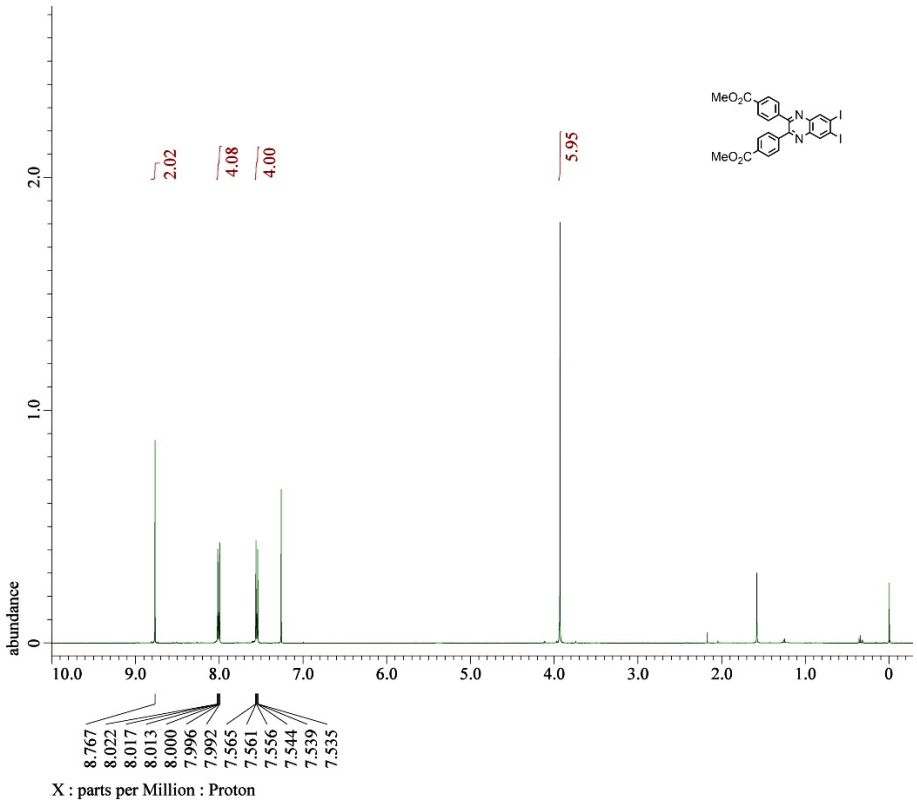

Figure S7. ^{1}H NMR (400 MHz, $CDCl_3$) spectrum of diiodoquinoxaline derivative **3**.

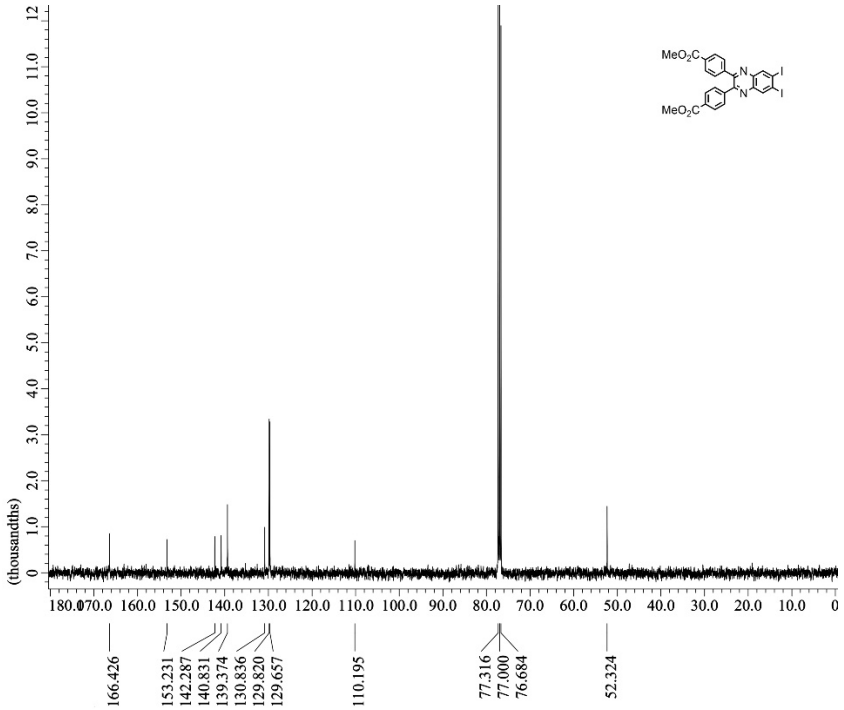

Figure S8. ^{13}C NMR (100 MHz, $CDCl_3$) spectrum of diiodoquinoxaline derivative **3**.

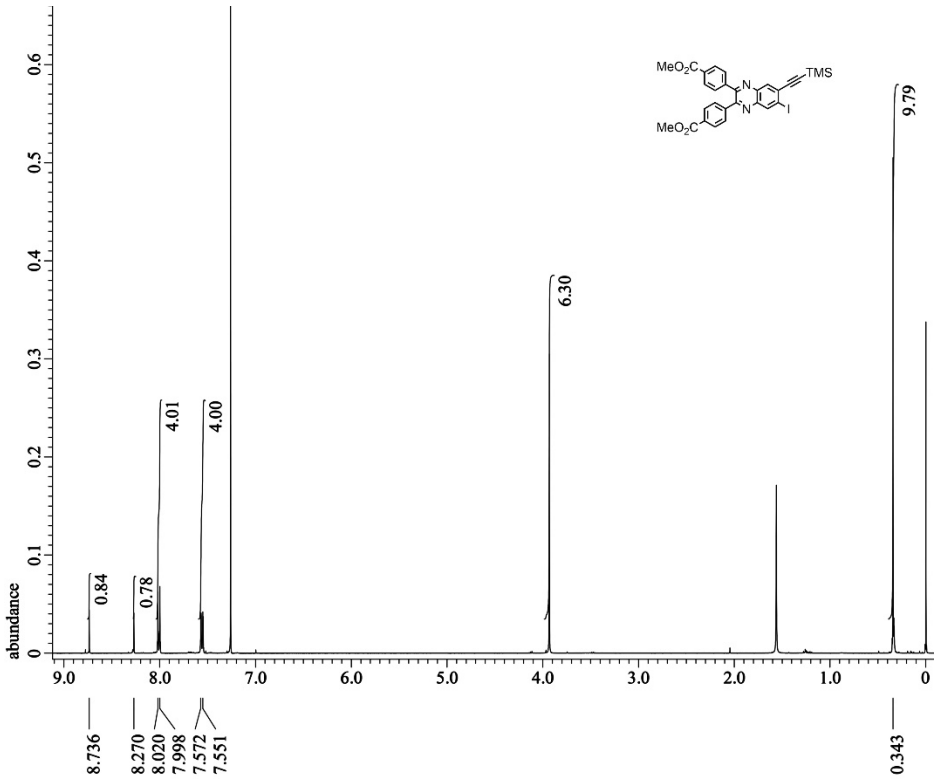

Figure S9. ^{1}H NMR (400 MHz, $CDCl_3$) spectrum of phenylethynyl derivative **4**.

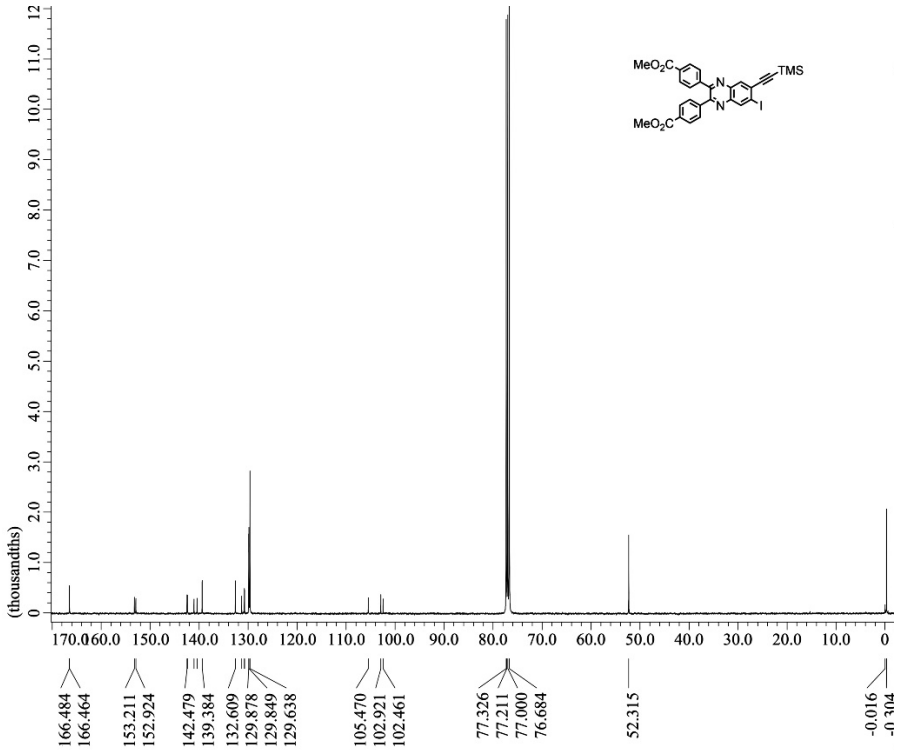

Figure S10. ^{13}C NMR (100 MHz, $CDCl_3$) spectrum of phenylethynyl derivative **4**.

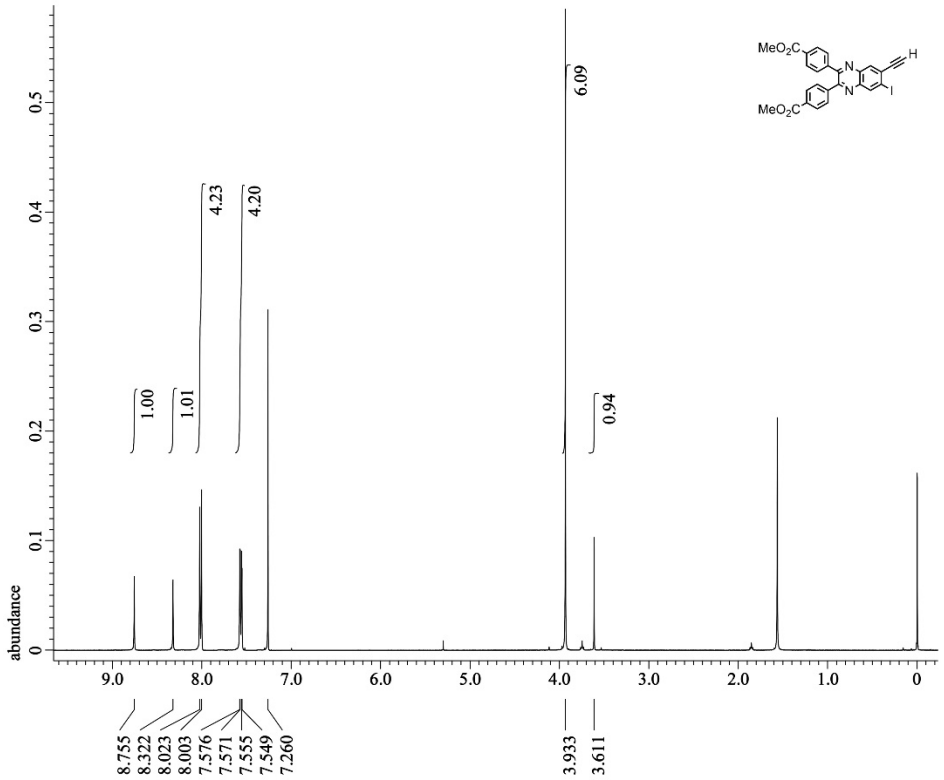

Figure S11. ^{1}H NMR (400 MHz, $CDCl_3$) spectrum of terminal acetylene **4a**.

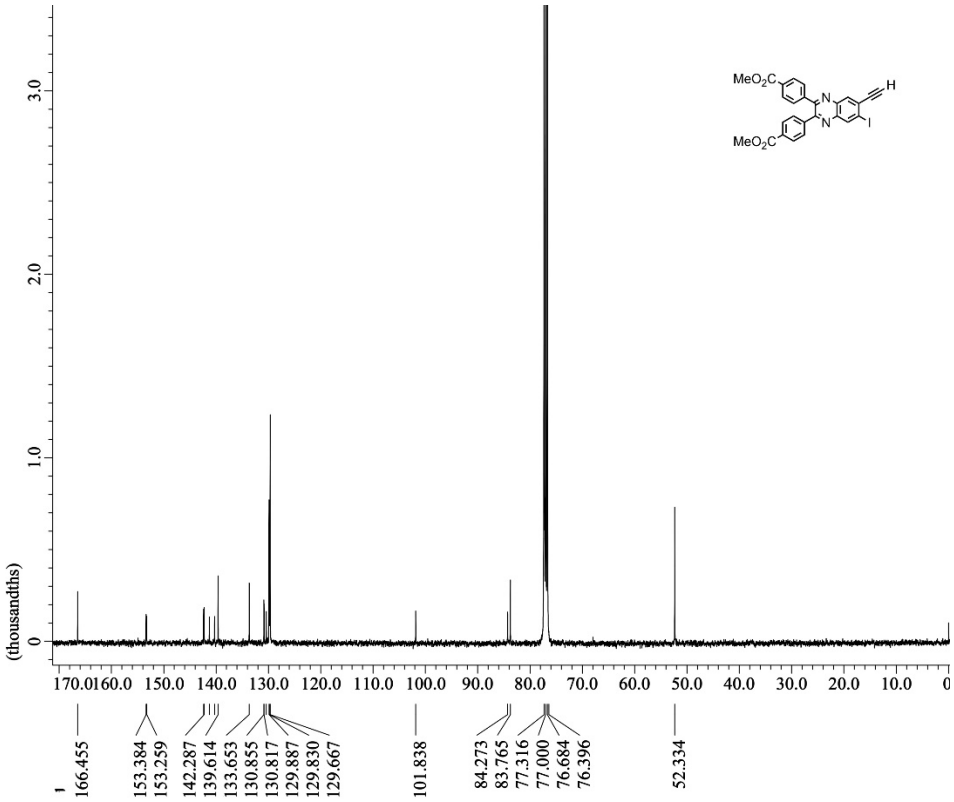

Figure S12. ^{13}C NMR (100 MHz, $CDCl_3$) spectrum of terminal acetylene **4a**.

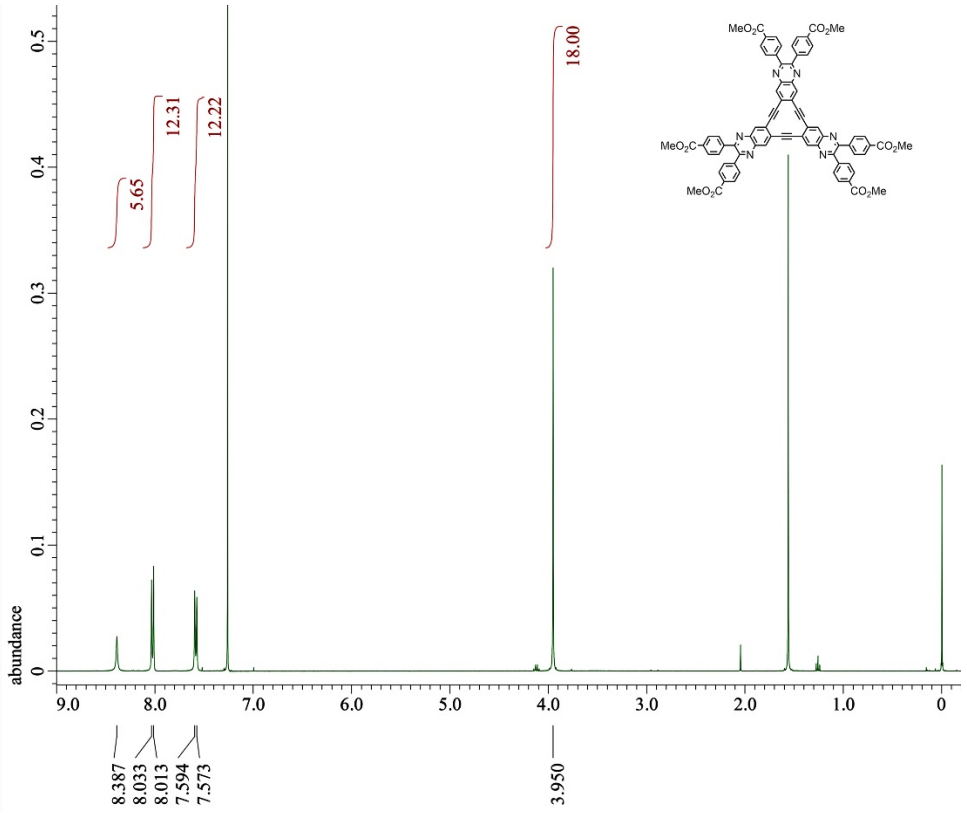

Figure S13. ^{1}H NMR (400 MHz, $CDCl_3$) spectrum of dehydro[12]annulene derivative **5**.

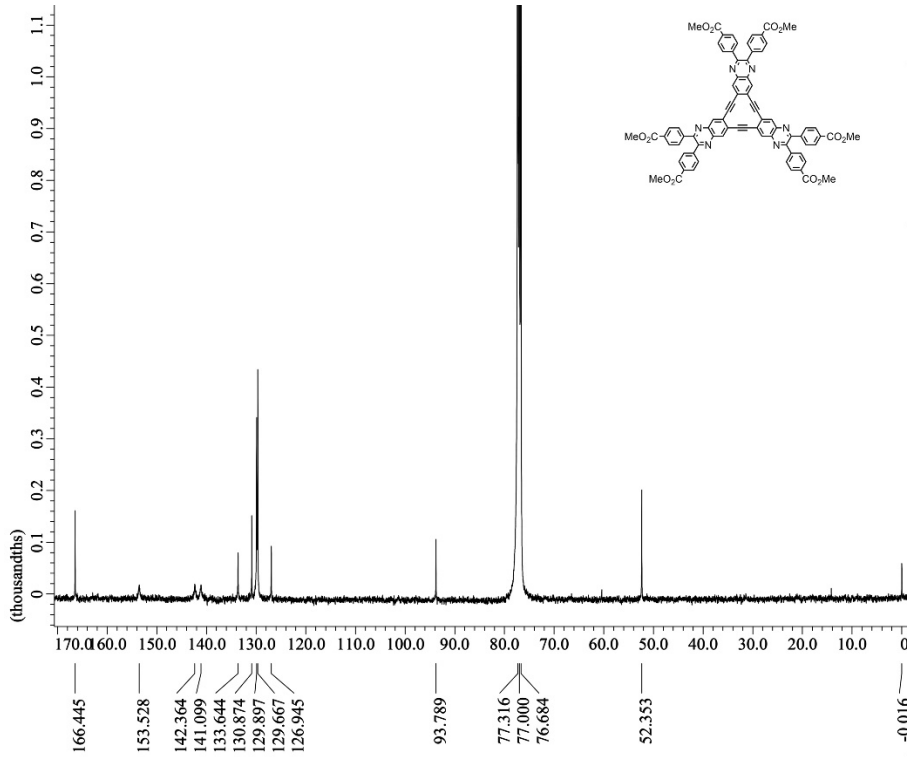

Figure S14. ^{13}C NMR (100 MHz, $CDCl_3$) spectrum of dehydro[12]annulene derivative **5**.

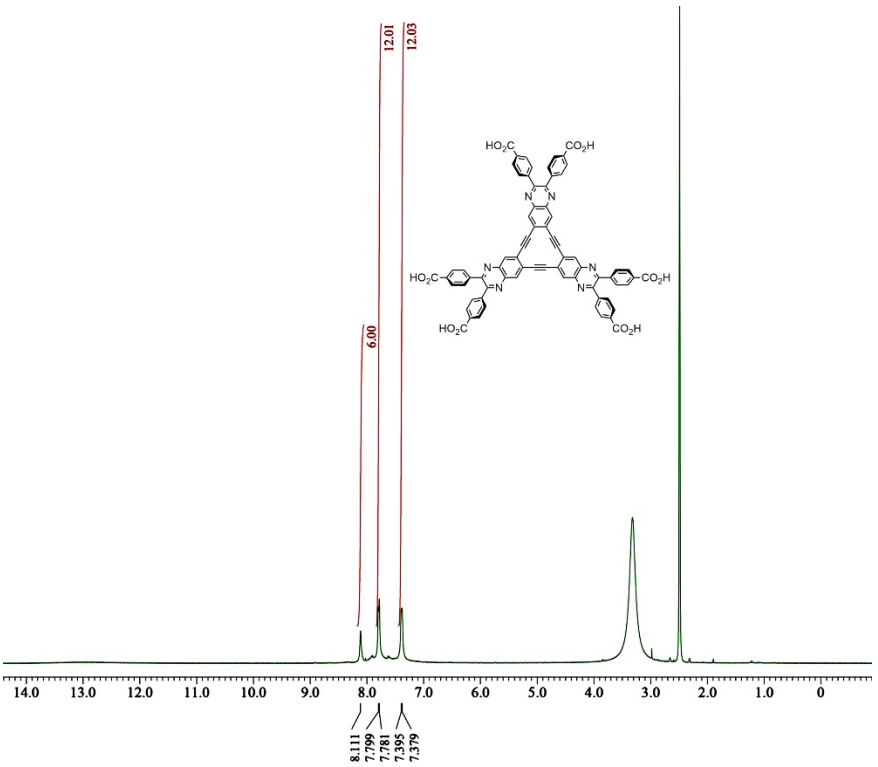

Figure S15. ^{1}H NMR (400 MHz, DMSO-d_6) spectrum of **TQ12**.

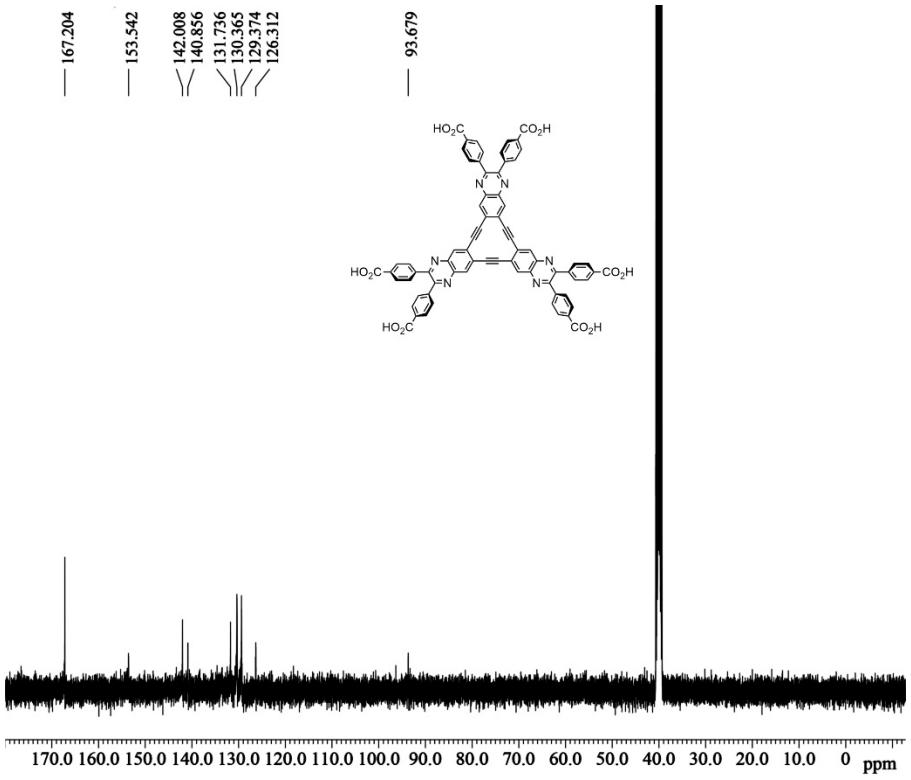

Figure S16. ^{13}C NMR (100 MHz, DMSO-d_6) spectrum of **TQ12**.

9. References

S1. Gaussian 09, Revision A.02, M. J. Frisch, G. W. Trucks, H. B. Schlegel, G. E. Scuseria, M. A. Robb, J. R. Cheeseman, G. Scalmani, V. Barone, G. A. Petersson, H. Nakatsuji, X. Li, M. Caricato, A. Marenich, J. Bloino, B. G. Janesko, R. Gomperts, B. Mennucci, H. P. Hratchian, J. V. Ortiz, A. F. Izmaylov, J. L. Sonnenberg, D. Williams-Young, F. Ding, F. Lipparini, F. Egidi, J. Goings, B. Peng, A. Petrone, T. Henderson, D. Ranasinghe, V. G. Zakrzewski, J. Gao, N. Rega, G. Zheng, W. Liang, M. Hada, M. Ehara, K. Toyota, R. Fukuda, J. Hasegawa, M. Ishida, T. Nakajima, Y. Honda, O. Kitao, H. Nakai, T. Vreven, K. Throssell, J. A. Montgomery, Jr., J. E. Peralta, F. Ogliaro, M. Bearpark, J. J. Heyd, E. Brothers, K. N. Kudin, V. N. Staroverov, T. Keith, R. Kobayashi, J. Normand, K. Raghavachari, A. Rendell, J. C. Burant, S. S. Iyengar, J. Tomasi, M. Cossi, J. M. Millam, M. Klene, C. Adamo, R. Cammi, J. W. Ochterski, R. L. Martin, K. Morokuma, O. Farkas, J. B. Foresman, and D. J. Fox, Gaussian, Inc., Wallingford CT, 2016.

S2. G. M. Sheldrick, *Acta Crystallogr. Sect. A*, 2015, **71**, 3–8.

S3. G. M. Sheldrick, *Acta Crystallogr. C*, 2015, **71**, 3–8.

S4. P. v. d. Sluis and A. L. Spek, *Acta Crystallogr. Sect. A*, 1990, **46**, 194. (b) A. L. Spek, *Acta Crystallogr. Sect. D*, 2009, **65**, 148–155

S5. I. Hisaki, Y. Suzuki, E. Gomez, Q. Ji, N. Tohnai, T. Nakamura and A. Douhal, *J. Am. Chem. Soc*., 2019, **141**, 2111–2121.